Journal of Inflammation Research

Dovepress
Taylor & Francis Group

Open Access Full Text Article

ORIGINAL RESEARCH

Fingolimod Suppresses NLRP3 Inflammasome Activation and Alleviates Oxidative Stress in Traumatic Brain Injury-Induced Acute Lung Injury

Qi Shi[1,*], Tingting Hu[2,*], Lixia Xu[2,*], Jiayuanyuan Fu[1], Yehong Fang[1], Yu Lan[1], Weijia Fan[2], Qiaoli Wu[2], Xiaoguang Tong[1–3], Hua Yan[1–3]

[1]Clinical College of Neurology, Neurosurgery and Neurorehabilitation, Tianjin Medical University, Tianjin, 300070, People's Republic of China; [2]Tianjin Key Laboratory of Cerebral Vascular and Neurodegenerative Diseases, Tianjin Neurosurgical Institute, Tianjin Huanhu Hospital, Tianjin, 300350, People's Republic of China; [3]Department of Neurosurgery, Tianjin Huanhu Hospital, Tianjin, 300350, People's Republic of China

*These authors contributed equally to this work

Correspondence: Hua Yan, Clinical College of Neurology, Neurosurgery and Neurorehabilitation, Tianjin Medical University, Tianjin, 300070, People's Republic of China, Email yanh2023@tmu.edu.cn

Background: Acute lung injury (ALI) is a serious yet common complication in patients with traumatic brain injury (TBI), often associated with poor prognosis. The development of TBI-induced ALI is closely associated with excessive oxidative stress and NLRP3 inflammasome activation. Fingolimod, an immunomodulatory agent, has been reported to attenuate inflammatory responses, restore blood-brain barrier integrity, reduce cerebral edema, and mitigate associated neurological deficits.

Objective: This study aimed to investigate the mechanistic role of NLRP3 inflammasome activation in TBI-induced ALI and to evaluate the therapeutic potential of fingolimod in targeting this inflammatory pathway.

Results: A rat TBI model was established using the classical free-fall method, and animals were treated with fingolimod (0.5 or 1 mg/kg) daily for three days. The TBI model rats presented with clear signs of histopathological pulmonary damage, an increase in the permeability of capillaries in the lung, and pulmonary edema that coincided with significantly increased NLRP3, caspase-1, and ASC expression in lung tissue samples. This overexpression of NLRP3 inflammasome machinery resulted in the release of IL-1β. Fingolimod treatment, however, reversed all of these effects such that it suppressed NLRP3 activity and normalized levels of IL-1β, leading to the alleviation of inflammation. In line with these results, LPS and nigericin (NLRP3 agonist)-treated NR8383 cells treated using fingolimod exhibited reductions in reactive oxygen species production and NLRP3 inflammasome activation.

Conclusion: These findings suggest that NLRP3 inflammasome activation and oxidative stress are key mediators of TBI-induced ALI. Fingolimod exerts protective effects against this condition by inhibiting NLRP3 inflammasome activation, highlighting its potential as a therapeutic agent for TBI-associated pulmonary complications.

Keywords: traumatic brain injury, acute lung injury, fingolimod, NLRP3 inflammasomes, reactive oxygen species

Introduction

Traumatic brain injury (TBI) poses a significant global public health challenge, contributing to high morbidity and mortality rates while imposing significant socioeconomic burdens.[1,2] The management of both primary TBI and its secondary complications remains complex, often resulting in poor prognostic outcomes.[3] In TBI, the central nervous system (CNS) sustains a primary injury that can, in turn, activate the host immune response and trigger secondary damage both within the CNS and in the periphery.[4] After the incidence of TBI, brain-lung interactions have been damaged,[5] with TBI contributing to the exacerbation of pulmonary dysfunction.[6] Acute lung injury (ALI) is a complication that is often observed in patients suffering from sustained TBI,[7] and impaired respiratory function is generally associated with poor post-TBI outcomes.[8] Neurogenic pulmonary edema (NPE) is a condition characterized by the rapid accumulation of fluid in the alveoli and pulmonary interstation after damage to the CNS that is generally

Received: 29 October 2024
Accepted: 8 February 2025
Published: 14 February 2025

Graphical Abstract

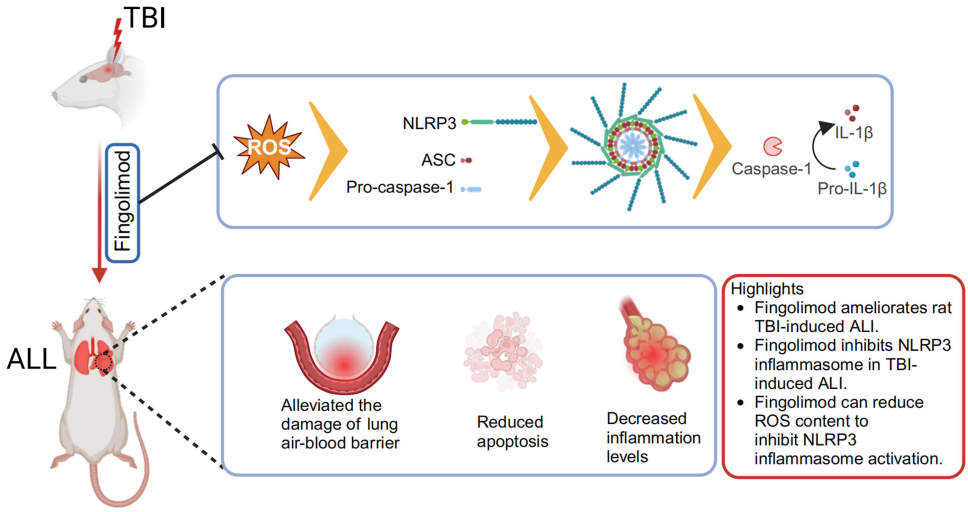

thought to be a consequence of cardiorespiratory dysfunction.[9] NPE has been reported in patients with TBI, spinal cord injury, intracranial hemorrhage, and subarachnoid hemorrhage.[10] Emerging evidence suggests that post-TBI pulmonary inflammation is a key driver of lung injury, contributing to disease progression.[11]

The nucleotide-binding oligomerization domain (NOD)-like receptor (NLR) protein family, particularly NLRP3, plays a central role in recognizing pathogens, cellular stress signals, and exogenous or endogenous damage-associated molecular patterns.[12] When NLRP3 activity is triggered by factors such as reactive oxygen species (ROS), this protein forms a complex with apoptosis-associated speck-like protein (ASC) and pro-caspase-1, and this inflammasome complex culminates in caspase-1 activation and the secretion of mature interleukin (IL)-1β.[13] Many studies have demonstrated a key role for NLRP3 inflammasome signaling in the pathogenesis of TBI-induced ALI.[7,14,15] Specifically, this condition is exacerbated by pulmonary NLRP3 inflammasome activity triggered in response to TBI incidence.[7] Furthermore, Kerr et al[16] proposed a "neural-respiratory-inflammasome axis", highlighting the broader involvement of inflammasome-mediated signaling in the pathogenesis of TBI-induced ALI. Targeted inhibition of the NLRP3 inflammasome has shown promise in mitigating this condition.[17] MCC950 is a small molecule compound that inhibits NLRP3 with a high degree of selectivity.[18] The therapeutic potential of inflammasome-targeting agents has been explored across major organs, including the heart and brain,[19] prompting ongoing research to develop safer and more effective inhibitors for clinical application in TBI-induced ALI.

Fingolimod, a non-selective sphingosine-1-phosphate (S1P) receptor agonist, has been approved by the US Food and Drug Administration (FDA) for the treatment of multiple sclerosis.[20] Moreover, numerous studies have demonstrated the effectiveness of fingolimod in treating various diseases of the nervous system, including intracerebral hemorrhage, ischemic stroke, Huntington's disease, Alzheimer's disease, epilepsy, and spinal cord injury.[21–26] In addition to its ability to preserve or restore the integrity of the blood-brain barrier (BBB) and to interfere with neuroinflammation, fingolimod can also reportedly facilitate post-TBI neurological functional recovery.[27] Many studies have confirmed the protective effects of fingolimod and analogs in the lungs in different ALI models.[28–30] These beneficial effects are attributable to improved pulmonary endothelial barrier function and a decrease in the leakage of the pulmonary vasculature.[29] Fingolimod has recently been demonstrated to benefit some multiple sclerosis patients through its ability to suppress inflammasome signaling.[31] In rodent Parkinson's disease and chronic unpredictable mild stress models, it can similarly inhibit the NLRP3 inflammasome to reduce microglial activation.[32,33] In light of the ability of fingolimod to serve as an NLRP3 inflammasome inhibitor, its potential ability to alleviate TBI-induced ALI through this mechanism was investigated in this study.

Materials and Methods

Reagents

The reagents used for this study included: Fingolimod (HY-12005, MedChemExpress), Lipopolysaccharide (LPS, L2630, Sigma-Aldrich), Nigericin (B24364, Shanghai yuanye Bio-Technology Co., Ltd), MCC950 (538120, Sigma-Aldrich), Evans blue dye (E8010, Solaribo), DAB (ZLI-9018, ZSGB-BIO), RIPA buffer (R0278, Sigma-Aldrich), and dihydroethidium (DHE, 38483–26-0, Aladdin). Utilized antibodies were specific for: β-actin (B1029, Biodragon), Phospho-NF-κB p65 (82,335-1-RR, Proteintech), caspase-1 (22,915-1-AP, Proteintech), NLRP3 (A5652, ABclonal), ASC (67494-1-Ig, Proteintech), iNOS (ab178945, Abcam), IL-1β (sc-515598, Santa Cruz Biotechnology), cleaved caspase-3 (9661, Cell Signaling Technology), Bax (2772S, Cell Signaling Technology), Bcl-xl (2764S, Cell Signaling Technology), Claudin-1 (ab15098, Abcam), occludin (13409-1-AP, Proteintech), CD68 (14–0688-82, Invitrogen), and SFTPC (sc-518029, Santa Cruz Biotechnology). ROS (S0033S) and TUNEL (C1086) assay kits, as well as DAPI (P0131) were from Beyotime, while BSA (A8020) was from Solarbio, and TNF-α (MM-0180R1), IL-6 (MM-0190R1), and IL-1β (MM-0047R1) ELISA kits were from Jiangsu Meimian Industrial Co., Ltd.

Animals

Male Sprague-Dawley (SD) rats (6–8 weeks old, 280–320 g) were obtained from SPF Biotechnology (Beijing, China) (certificate: SCXK (Jing) 2019–0010). All animal procedures were conducted following the NIH Guidelines for the Care and Use of Laboratory Animals and were approved by the Institutional Animal Care Committee of Tianjin Huanhu Hospital (Approval No.: HHYY-2024-001). The rats were housed under controlled conditions, including a temperature of 23°C, 50% humidity, and a 12-hour light/dark cycle within a specific pathogen-free facility. They had *ad libitum* access to standard chow, tap water, or designated experimental solutions. A seven-day acclimatization period was provided before the initiation of experiments.

TBI Modeling and Treatment

A classical free-fall model was used for rat TBI modeling.[34] Briefly, rats were anesthetized with pentobarbital (50 mg/kg), after which the surgical site was sterilized. A longitudinal incision was made along the skull midline, and the animals were secured to a stereotaxic apparatus using nose forceps and two ear rods. A 400 g cylindrical metal hammer was dropped vertically from a height of 45 cm through a guided tube, impacting the left cerebral hemisphere 1 mm anterior to the coronal suture and 2 mm lateral to the midline. Sham control rats underwent only a skin incision without TBI induction. The incised area was cleaned after surgery, and the wound was sutured. Rats were then placed in a heated cage to facilitate anesthesia recovery and maintain appropriate body temperature.

Rats in this study were assigned to seven experimental groups at random (n = 5/group), including (I) sham controls, (II) TBI model rats, (III) TBI + vehicle treatment, (IV) TBI + 0.5 mg/kg fingolimod, (V) TBI + 1 mg/kg fingolimod, (VI) TBI + 3 mg/kg MCC950, and (VII) TBI + 0.5 mg/kg fingolimod + 3 mg/kg MCC950. Fingolimod and MCC950 were dissolved in saline and intraperitoneally injected, as was saline as the vehicle control in respected rats. Rats in groups III–VII received appropriate treatments once daily for three days, after which samples were collected.

Lung Histopathology

Lung tissues were collected and fixed in 4% paraformaldehyde (PFA) for 24 hours, followed by paraffin embedding and sectioning at a thickness of 5 μm. The sections were stained with hematoxylin and eosin (H&E) and examined under a light microscope. Lung injury was assessed based on a previously established scoring system.[35] Briefly, 10 high-power fields (400×) were scored to assess: (1) Alveolar neutrophil infiltration, (2) Interstitial neutrophil infiltration, (3) Alveolar septal thickening, (4) Formation of a hyaline membrane, and (5) Whether proteinaceous debris was present in the alveoli. Lung injury levels were independently scored by two investigators blinded to experimental grouping.

Bronchoalveolar Lavage Fluid (BALF) Analyses

After rats had been euthanized, they were affixed to a foam board, and the trachea was exposed and incised, followed by the introduction of an indwelling needle that was secured using thread. The lungs were washed twice using 5 mL of cold saline, and BALF recovery rates were > 80%. Following centrifugation (10 min, 1500 g, 4°C), supernatant protein levels were analyzed, and IL-1β, IL-6, and TNF-α content was detected via ELISA.

Pulmonary Edema Measurements

To evaluate the severity of pulmonary edema, intact lungs were excised from exsanguinated animals and immediately weighed to determine the wet weight. The lungs were then dried in an oven at 98°C for 48 h or until a constant weight was achieved. The wet-to-dry weight ratio was then calculated as an index of lung water content.

Lung Capillary Leakage Analyses

Pulmonary vascular permeability was assessed using Evans blue dye leakage.[36] Briefly, rats were intravenously injected via the tail vein with 2% Evans blue dye in saline (5 mL/kg) 2 h before euthanasia. After perfusion, the lungs were excised and homogenized in 0.5 mL of formamide, followed by incubation at 60°C for 18 h. The homogenates were centrifuged at 5000 × g for 30 min, and the absorbance of Evans blue dye in the supernatants was measured at 610 nm. A standard curve was generated for quantitative analysis.

TUNEL Assay

A TUNEL kit was used as directed to assess cellular apoptosis. Briefly, lung tissue sections were stained for 1 h at 37°C with the TUNEL reaction mixture, followed by DAPI counterstaining for 10 min and the subsequent visualization of these sections with a last confocal microscopy.

Immunohistochemistry (IHC)

Tissue sections were deparaffinized using xylene and rehydrated through a graded ethanol series. Antigen retrieval was performed by heating the samples in a pressure cooker at 121°C for 4 min in 10 mm citrate buffer (pH 6.0), followed by cooling to room temperature. Endogenous peroxidases were inactivated using 5% hydrogen peroxide (H□O□), and nonspecific binding was blocked with 5% bovine serum albumin (BSA) for 1 h. Samples were then incubated overnight at 4°C with anti-occludin primary antibodies (1:500), followed by staining with secondary antibodies (1:1000). The signal was developed using 3.3′-diaminobenzidine (DAB) and occludin-positive cells were quantified using a light microscope.

Western Immunoblotting

After using RIPA buffer with protease and PhosphoSTOP phosphatase inhibitor tablets to homogenize samples in a JXFSTPRP tissue homogenizer (Sonics, USA), protein content was measured via BCA assay, and 50–75 μg per sample was separated by SDS-PAGE and transferred to a PVDF blot. After blocking and incubating with anti-IL-1β (1:500), anti-caspase 1 (1:2000), anti-ASC (1:5000), anti-p-NF-κB (1:2000), anti-cleaved-caspase 3 (1:1000), anti-Bcl-xl (1:1000), anti-Bax (1:1000), anti-Claudin 1 (1:200), anti-Occludin (1:5000), anti-NLRP3 (1:1000), anti-iNOS (1:500), or anti-β-actin (1:10000) overnight at 4°C, secondary antibodies (1:10000) were applied, followed by the use of an Odyssey® CLX (LI-COR, USA) to perform densitometric analyses of the protein bands.

Immunofluorescence

Tissue sections were processed following the same steps as described for IHC staining up to the blocking step. Then, sections were incubated overnight at 4°C with primary antibodies against ASC (1:100), CD68 (1:100), SFTPC (1:100), and NLRP3 (1:100). The following day, sections were treated with secondary antibodies (1:500) for 90 min at room temperature in the dark. Nuclear counterstaining was performed using a Fluoroshield mounting medium containing

DAPI. Fluorescence imaging was conducted using a Zeiss LSM880 confocal microscope for both control and experimental groups under identical acquisition settings.

Cell Culture

The rat alveolar macrophage NR8383 cell line was purchased from Cellverse Bioscience Technology Co., Ltd. (Shanghai, China) and cultured in F12K containing 15% FBS at 37°C in a 5% CO_2 incubator.

ROS Analyses

ROS levels were assessed using the Beyotime ROS Assay Kit according to the manufacturer's instructions. Briefly, isolated cells were incubated with 10 μM DCFH-DA in PBS at 37°C for 20 minutes, followed by PBS washing and resuspension in the growth medium. Samples were then analyzed using flow cytometry. For in vivo ROS detection, DHE staining was performed as per standard protocols. Rats received an intraperitoneal injection of DHE (1 mg/mL) following appropriate treatments and myocardial perfusion was conducted after 1 h. Lungs were subsequently excised, fixed in 4% PFA overnight, and cryoprotected in PBS containing 30% sucrose. The lungs were then sectioned using a cryostat, incubated in PBS for 30 min, counterstained with DAPI-containing Fluoroshield mounting medium, and imaged using a confocal microscope under identical acquisition settings.

Statistical Analyses

All data analyses were performed using SPSS 21.0 and GraphPad Prism 9.0. Results were expressed as the mean ± standard error of the mean (SEM). Group comparisons were conducted using one-way analysis of variance (ANOVA) for normally distributed data, while the Kruskal–Wallis or other nonparametric tests were used for data that did not meet normality assumptions. A P-value of < 0.05 was considered statistically significant.

Results

Fingolimod Alleviates Histopathological Changes, Decreases Pulmonary Vascular Permeability, and Reduces Pulmonary Water Content in TBI-Induced ALI

Fingolimod has been extensively used in rat models of TBI, with previous studies demonstrating the efficacy of both low (0.5 mg/kg) and high (1 mg/kg) doses without inducing toxic side effects (Figure 1A).[37–39] TBI pathogenesis was characterized by contusions, cerebral congestion, and swelling at the zone of impact (Figure 1B). Histopathological analysis of lung tissues from TBI model rats revealed significant pulmonary parenchymal alterations, including alveolar wall thickening, inflammatory cell infiltration into the interstitial layer, hyaline membrane formation, and intra-alveolar exudate accumulation—features absent in sham controls (Figure 1C). On day 3 post-TBI, semiquantitative analyses revealed more severe lung damage in these TBI model animals (Figure 1D). To further determine the degree of lung injury, BALF protein content, and Evans blue dye leakage were used to quantify lung permeability, both of which were elevated in the TBI model group relative to the sham group (Figure 1E-G). To detect pulmonary edema, lung weight/dry ratios were also quantified and found to be significantly higher in the TBI group relative to sham rats (Figure 1H), confirming the successful establishment of the TBI model. Fingolimod treatment at both doses (0.5 and 1 mg/kg) significantly mitigated histopathological lung damage (Figure 1C and D), reduced vascular leakage (Figure 1E–G), and lowered pulmonary water content (Figure 1H) in TBI model rats.

Fingolimod Significantly Alleviates Post-TBI Pulmonary Apoptosis

To test the impact of fingolimod on the lungs, TUNEL staining and Western immunoblotting were next performed on day 3 post-TBI. A pronounced increase in TUNEL-positive cells was noted in the TBI group relative to the sham group at this time point, whereas both tested fingolimod doses significantly decreased apoptotic cell numbers (Figure 2A and B). Western immunoblotting also demonstrated that TBI triggered the expression of higher levels of apoptosis-related Bax and cleaved caspase-3, while the opposite was true for anti-apoptotic Bcl-xl, and fingolimod reversed these changes in pulmonary apoptotic protein expression (Figure 2C –F).

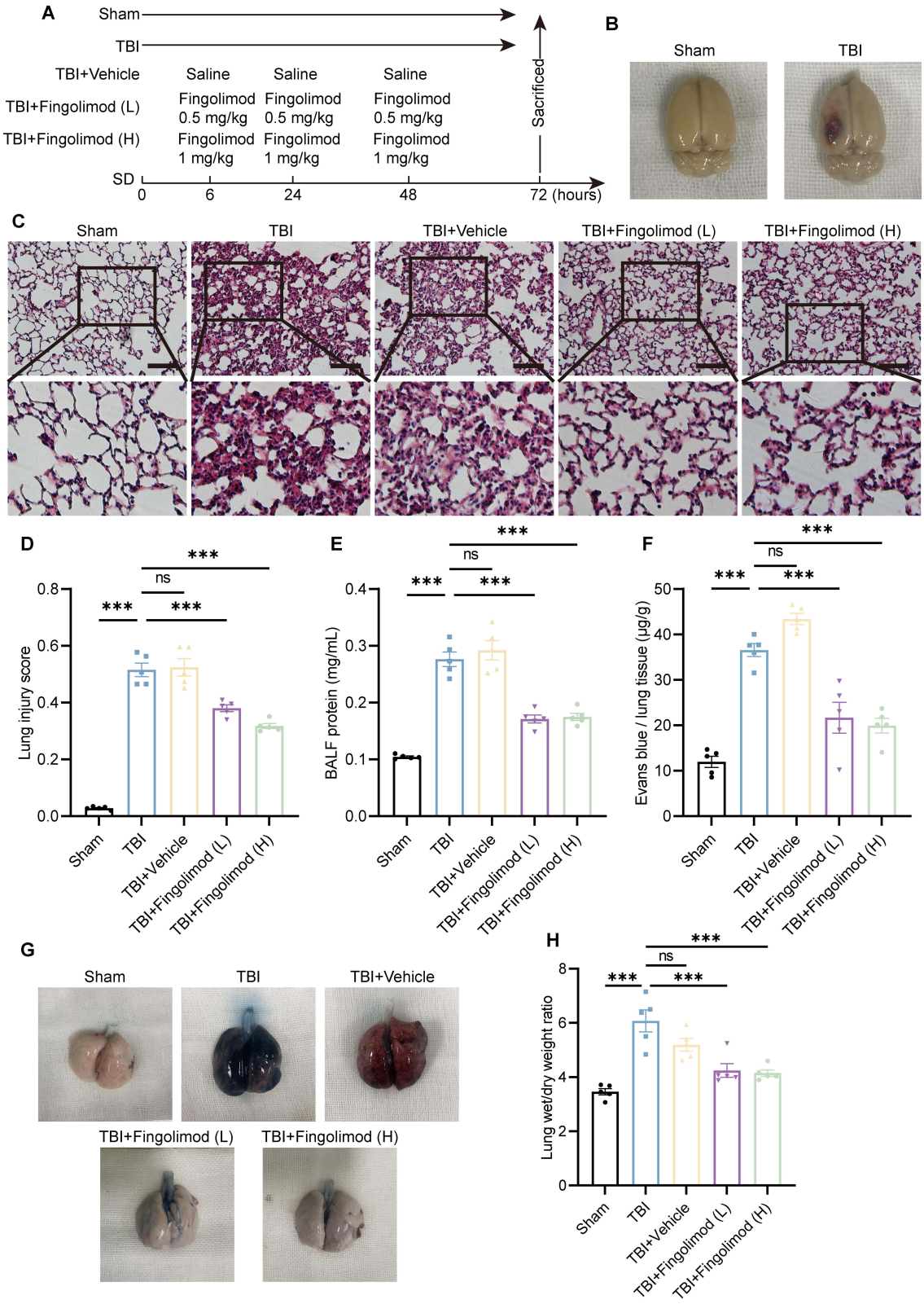

Figure 1 Effects of fingolimod on pulmonary symptoms following traumatic brain injury (TBI). (**A**) Experimental procedure in rats. (**B**) Gross observation of the brain. (**C**) Representative hematoxylin and eosin (HE)-stained lung tissue sections for histological evaluation; scale: 100 μm. (**D**) Pathological scores of lung tissue. (**E**) Total protein concentration in bronchoalveolar lavage fluid (BALF). (**F**) Evans blue dye concentration in lung tissue. (**G**) Gross observation of lung tissue with Evans blue staining, indicating vascular leakage in rats. (**H**) Lung wet/dry weight ratio. Values represent mean ± SEM. Statistical comparisons were performed using one-way ANOVA. ***$P < 0.001$; ns, not significant. n = 5. Fingolimod (L), 0.5 mg/kg; Fingolimod (H), 1 mg/kg.

https://doi.org/10.2147/JIR.S503428

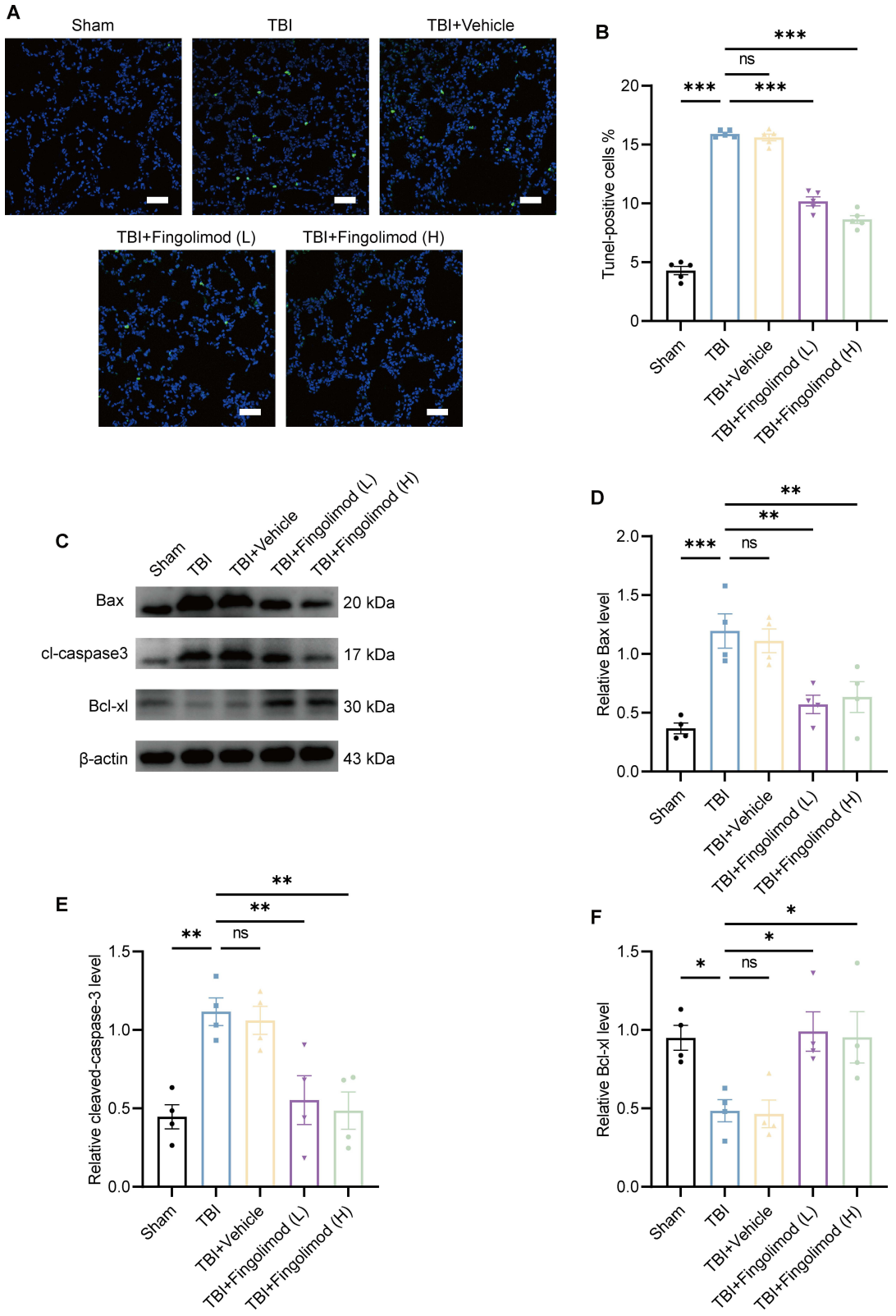

Figure 2 Effects of fingolimod on apoptosis in lung tissue following TBI. (**A** and **B**) Representative images of TUNEL fluorescence staining and quantification of TUNEL-positive cells; scale: 50 μm (n = 5). (**C**) Representative Western blots of Bax, Bcl-xl, and cleaved caspase-3 expression in lung tissue. (**D–F**) Western blot analysis and densitometric quantification of Bax, Bcl-xl, and cleaved caspase-3 in lung tissue (n = 4). Values represent mean ± SEM. Statistical comparisons were performed using one-way ANOVA. **P* < 0.05; ***P* < 0.01; ****P* < 0.001; ns, not significant. Fingolimod (L), 0.5 mg/kg; Fingolimod (H), 1 mg/kg.

https://doi.org/10.2147/JIR.S503428

Fingolimod Mitigates Blood-Air Barrier Damage in the Context of TBI-Induced ALI

The blood-air barrier in the lungs was next evaluated with a focus on tight junction protein expression through IHC and Western immunoblotting approaches. Both claudin-1 and occludin expression levels were reduced after TBI in the lungs of model rats (Figure 3A–E), whereas fingolimod reversed these changes in pulmonary tight junction protein expression (Figure 3A–E). Based on these data, fingolimod appears to be capable of beneficially affecting the blood-air barrier, protecting against TBI-associated dysfunction.

Fingolimod Reduces the Severity of Pulmonary TBI-Induced Inflammation in Lung Tissue

The anti-inflammatory effects of fingolimod in post-TBI pulmonary injury were further investigated by assessing inflammatory mediator levels in BALF and lung tissues using ELISAs and Western blot analysis. TBI model rats showed

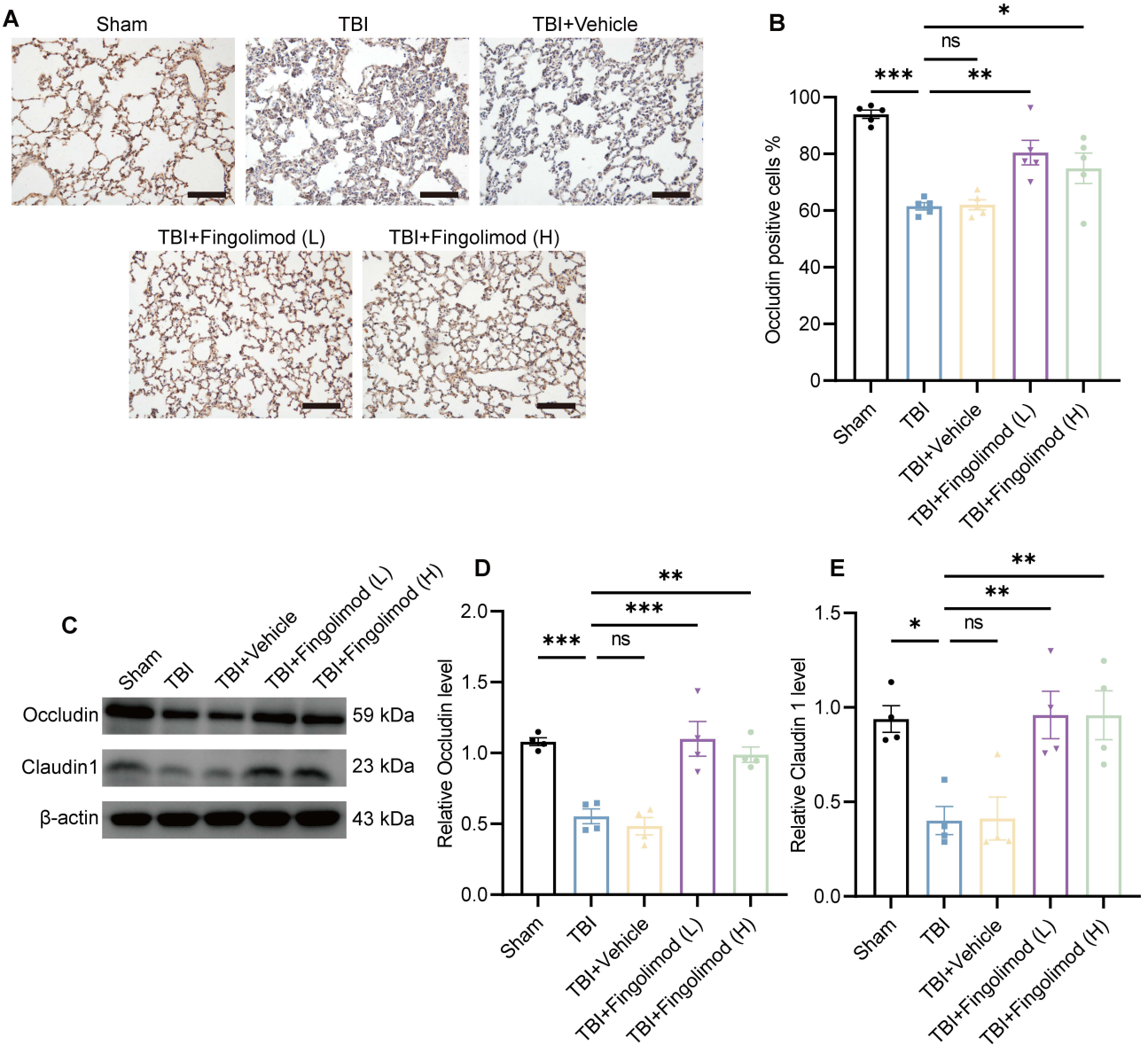

Figure 3 Effects of fingolimod on the lung air-blood barrier following TBI. (**A** and **B**) Representative images of occludin immunohistochemical (IHC) staining and quantification of occludin-positive cells; scale: 100 μm (n = 5). (**C**) Representative Western blots of occludin and claudin-1 expression in lung tissue. (**D** and **E**) Western blot analysis and densitometric quantification of occludin and claudin-1 in lung tissue (n = 4). Values represent mean ± SEM. Statistical comparisons were performed using one-way ANOVA. *$P < 0.05$; **$P < 0.01$; ***$P < 0.001$; ns, not significant. Fingolimod (L), 0.5 mg/kg; Fingolimod (H), 1 mg/kg.

 https://doi.org/10.2147/JIR.S503428

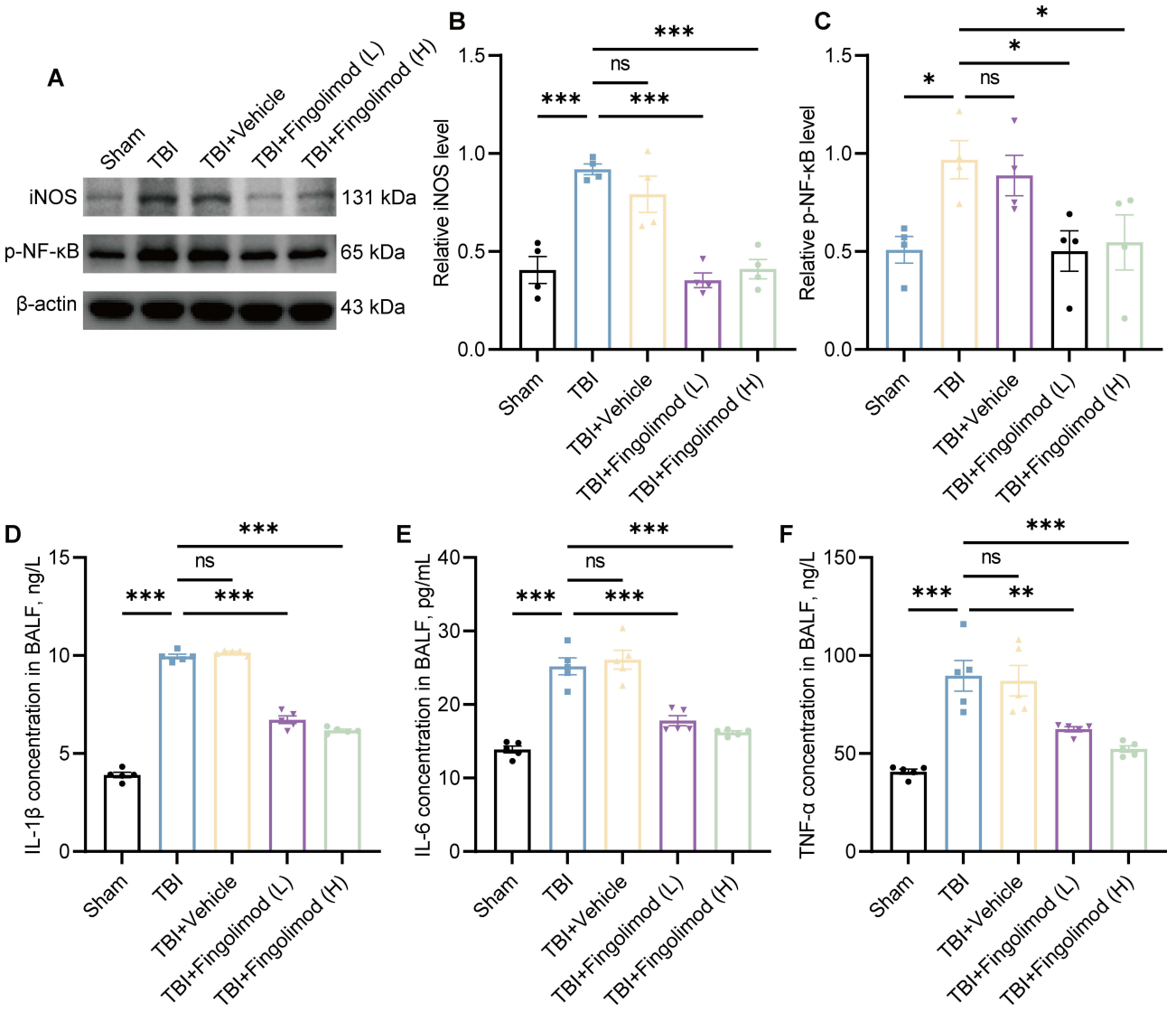

Figure 4 Effects of fingolimod on pulmonary inflammation following TBI. (**A**) Representative Western blots of iNOS and phospho-NF-κB expression in lung tissue. (**B** and **C**) Western blot analysis and densitometric quantification of iNOS and phospho-NF-κB in lung tissue (n = 4). (**D–F**) Quantitative assessment of (**D**) IL-1β, (**E**) IL-6, and (**F**) TNF-α concentrations in BALF samples using ELISA (n = 5). Values represent mean ± SEM. Statistical comparisons were performed using one-way ANOVA. **P* < 0.05; ***P* < 0.01; ****P* < 0.001; ns, not significant. Fingolimod (L), 0.5 mg/kg; Fingolimod (H), 1 mg/kg.

significantly increased expression of IL-1β, IL-6, TNF-α, iNOS, and p-NF-κB compared to sham controls. However, treatment with both low (0.5 mg/kg) and high (1 mg/kg) doses of fingolimod effectively reversed these inflammatory changes (Figure 4A–E). These findings indicate that fingolimod exerts a potent anti-inflammatory effect, significantly attenuating TBI-induced ALI-related lung inflammation.

Fingolimod Suppresses NLRP3 Inflammasome Activation in the Context of TBI-Induced ALI

Next, the impact of fingolimod on NLRP3 inflammasome-related protein levels was analyzed in the lungs of TBI model rats through immunofluorescent staining for NLRP3 (green) and ASC (red), with DAPI (blue) as a nuclear counterstain. TBI was associated with a significant increase in the numbers of pulmonary NLRP3- and ASC-positive cells (Figure 5A–C). Western immunoblotting also revealed significant increases in NLRP3, ASC, cleaved-caspase-1, and IL-1β levels in these TBI model rats (Figure 5D–H). These results support the activation of the NLRP3 inflammasome in the context of TBI-induced ALI. All of these inflammatory changes were reversed by fingolimod (0.5 or 1 mg/kg).

https://doi.org/10.2147/JIR.S503428

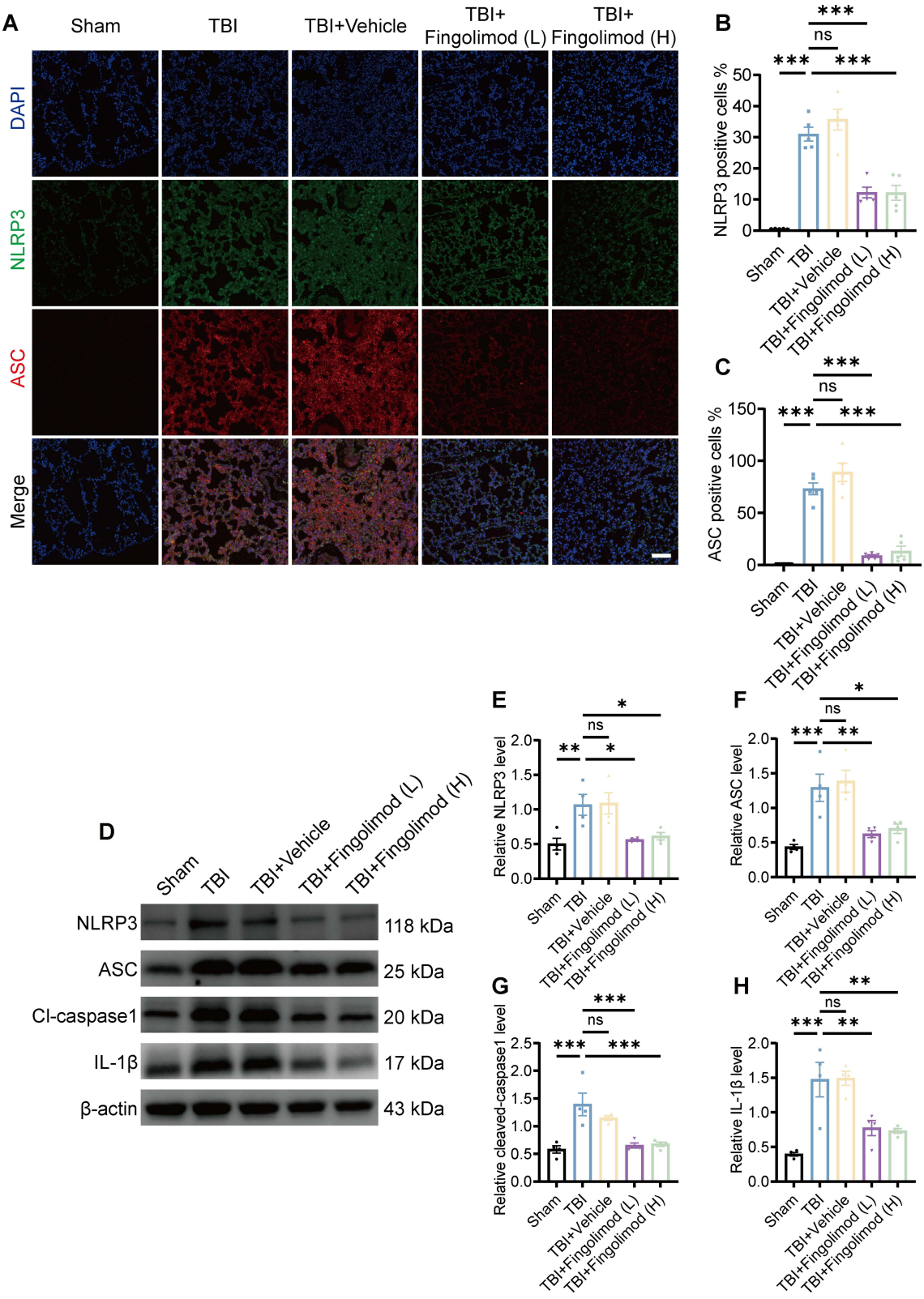

Figure 5 Effects of fingolimod on NLRP3 inflammasome-related proteins and cytokines in lung tissue following TBI. (**A–C**) Representative images of NLRP3 and ASC fluorescence staining and quantification of positive cells; scale: 50 μm (n = 5). (**D**) Representative Western blots of NLRP3, ASC, cleaved caspase-1, and IL-1β expression in lung tissue. (**E–H**) Western blot analysis and densitometric quantification of NLRP3, ASC, cleaved caspase-1, and IL-1β in lung tissue (n = 4). Values represent mean ± SEM. Statistical comparisons were performed using one-way ANOVA. **P* < 0.05; ***P* < 0.01; ****P* < 0.001; ns, not significant. Fingolimod (L), 0.5 mg/kg; Fingolimod (H), 1 mg/kg.

The effects of fingolimod on the NLRP3 inflammasome in lung tissues after TBI were further analyzed using immunofluorescence staining for NLRP3, CD68 (macrophage marker), and SFTPC (type II alveolar epithelial cell marker). The results showed that the expression of NLRP3 in macrophages was significantly raised in lung tissues after TBI, while these effects were reversed by fingolimod treatment. Meanwhile, there was no significant difference in NLRP3 expression in type II alveolar epithelial cells after TBI compared with the sham group. Interestingly, fingolimod treatment reduced the expression of NLRP3 in type II alveolar epithelial cells (Figure 6A and B). To further confirm the ability of fingolimod to modulate NLRP3 inflammasome activity, NR8383 cells were stimulated with LPS and nigericin to induce NLRP3 inflammasome activation. This treatment resulted in increased expression of NLRP3, ASC, cleaved caspase-1, pro-IL-1β, and IL-1β. However, fingolimod treatment effectively alleviated these changes, and this effect was significantly enhanced by MCC950, a selective NLRP3 inhibitor (Figure 6C–H). Collectively, these findings indicate that fingolimod mitigates TBI-induced ALI by disrupting the assembly and activation of the NLRP3 inflammasome.

Fingolimod Suppresses the Activity of the NLRP3 Inflammasome Through the Inhibition of ROS Generation

To elucidate the specific mechanisms underlying fingolimod-mediated suppression of the NLRP3 inflammasome, its effects on ROS production were assessed. Fingolimod exhibits potent antioxidant activity, while excessive ROS levels can trigger NLRP3 inflammasome activation. DHE staining is a sensitive tool for detecting superoxide ions in live tissues, fluoresces red upon oxidation, and serves as an indicator of overall free radical production. A significant increase in DHE fluorescence was observed in the TBI group compared to the sham control group, consistent with elevated ROS levels. NLRP3 inhibition significantly reduced DHE fluorescence intensity in rat lung tissues post-TBI. However, the TBI + fingolimod group showed lower DHE fluorescence intensities than the TBI + MCC950 group, and co-treatment with MCC950 and fingolimod did not further decrease ROS production (Figure 7A and B). The ability of fingolimod to suppress ROS generation was further investigated in NR8383 cells with NLRP3 inflammasome activation. Intracellular ROS levels were detected using 2′,7′-dichlorodihydrofluorescein diacetate (DCFH-DA) as a fluorescent probe via flow cytometry (Figure 7C). LPS- and nigericin-treated cells showed significantly increased DCFH-DA fluorescence, indicative of elevated ROS levels compared to control cells. Both MCC950 and fingolimod treatments effectively reduced this oxidative stress (Figure 7D). These findings suggest that fingolimod mitigates ROS production, thereby limiting the activation of the NLRP3 inflammasome.

Discussion

The therapeutic benefits of fingolimod as a treatment for immunological disorders have been attributed to its ability to promote the sequestration of circulating lymphocytes within lymphoid organs, leading to immunosuppressive outcomes.[40] Short-term sequential fingolimod treatment has been established to protect against brain damage and promote cognitive and neurological recovery while modulating immune and inflammatory activity in TBI.[27] Similar benefits have also been noted in settings of cerebral hemorrhage and acute ischemic stroke.[41,42] As most studies to date have focused on how TBI affects the brain, relatively little remains known of its impact on major organs in the periphery. Some studies have demonstrated interactive effects between the brain and these peripheral organs in the setting of brain injury.[43] Here, fingolimod was found for the first time to inhibit the activation of the NLRP3 inflammasome in the context of TBI-induced ALI, extending the utility of this drug as an anti-inflammatory therapeutic option.

The pathophysiology of brain-lung interactions following TBI is complex. It involves neurogenic pulmonary edema, inflammation, neurodegeneration, alterations in the levels of neurotransmitters, autoimmune responses, and dysfunction of the autonomic nervous system.[44] The exact mechanism underlying TBI-induced ALI is currently unknown. Previous studies have found that TBI associated with pulmonary edema increased the protein contents of the BALF and induced infiltration of inflammatory cells and the secretion of inflammatory factors in the lungs during the acute post-TBI phase.[36,45] Consistent with these findings, the present study observed significantly increased pulmonary vascular permeability, pulmonary edema, and elevated BALF protein levels three days post-TBI. Moreover, TBI induced a robust pulmonary inflammatory response, leading to increased expression of pro-inflammatory cytokines, including

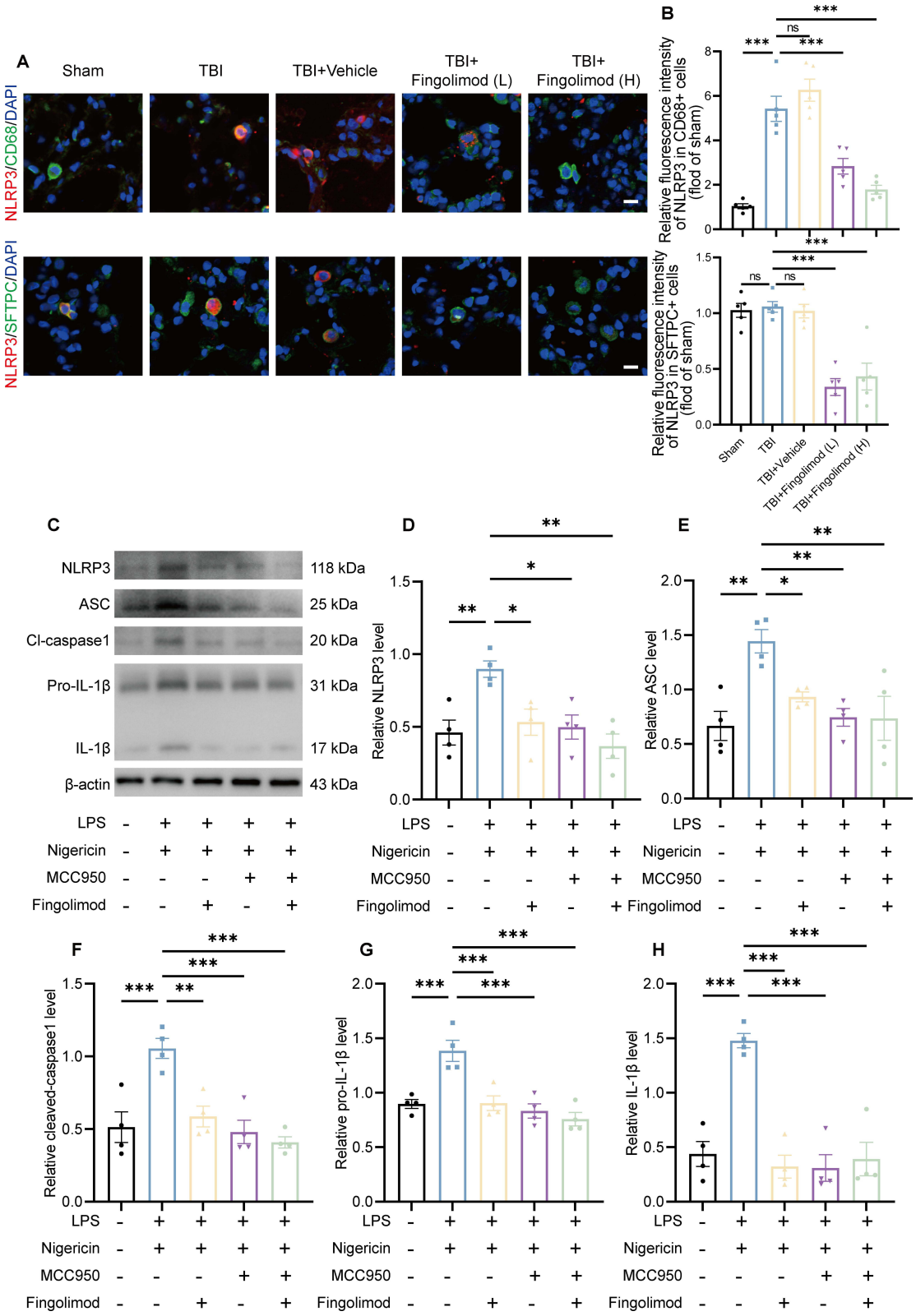

Figure 6 Effects of fingolimod on NLRP3 inflammasome-related proteins and cytokines in NR8383 cells. (**A**) Representative immunofluorescence images of NLRP3 (red), CD68 (green), and SFTPC (green) in rat lung tissue from different groups; scale: 10 μm. (**B**) Quantitative analysis of NLRP3 in various cell types (n = 5). (**C**) Western blot analysis of NLRP3 inflammasome components in NR8383 cells pre-treated with fingolimod (20 μM) and MCC950 (5 μM) for 12 hours before stimulation with LPS (1 μM) and nigericin (10 μM) for 3 hours. (**D–H**) Western blot analysis and quantification of (**D**) NLRP3, (**E**) ASC, (**F**) cleaved caspase-1, (**G**) pro-IL-1β, and (**H**) IL-1β expression (n = 4). Values represent mean ± SEM. Statistical comparisons were performed using one-way ANOVA. *P < 0.05; **P < 0.01; ***P < 0.001; ns, not significant.

https://doi.org/10.2147/JIR.S503428

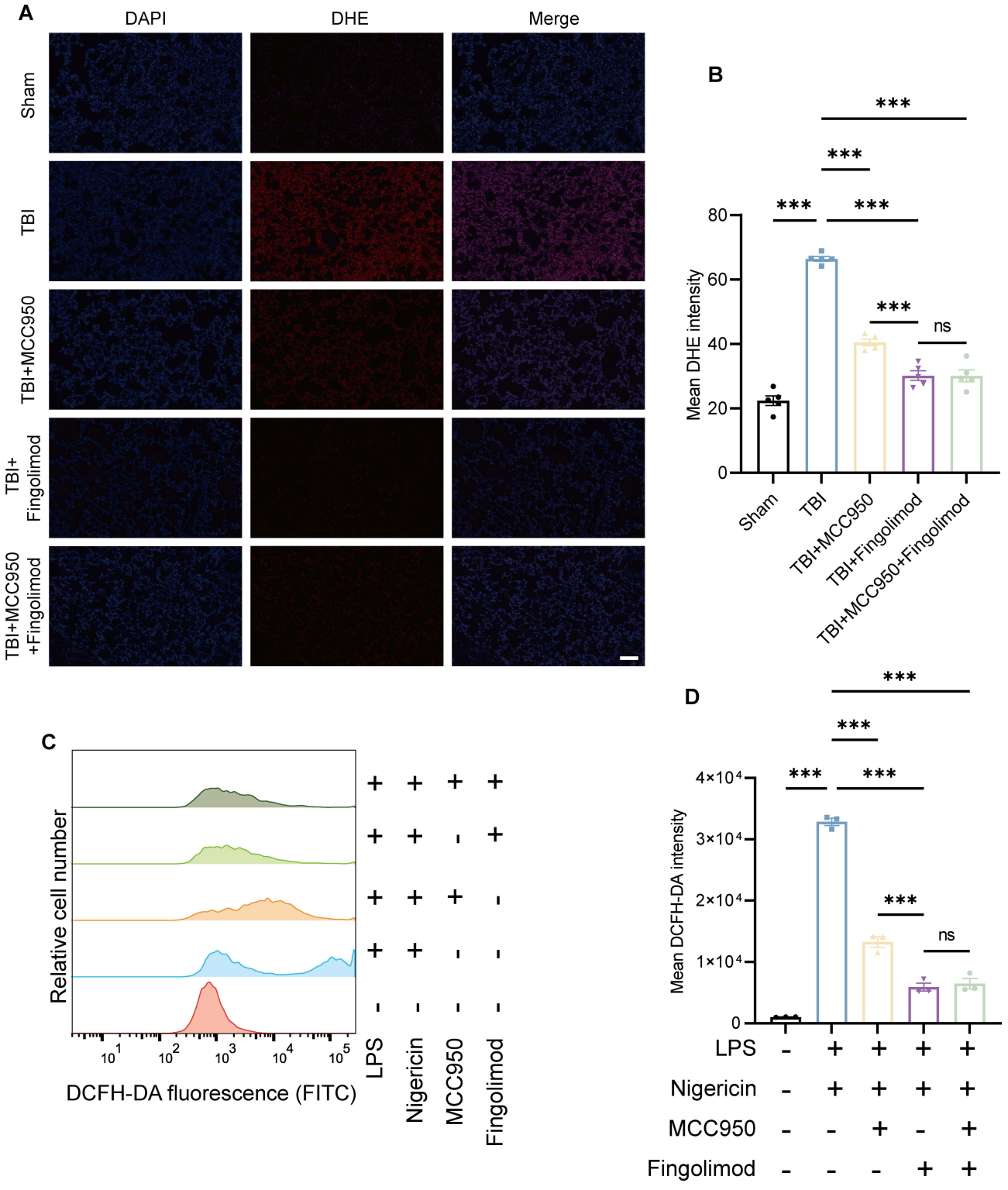

Figure 7 Effects of fingolimod on reactive oxygen species (ROS) production in vitro and in vivo. (**A**) Representative images of oxidized dihydroethidium (DHE) fluorescence staining in lung tissue from each group; scale: 100 μm. (**B**) Quantitative analysis of mean DHE fluorescence intensity (n = 5). (**C** and **D**) Effects of fingolimod on oxidative stress following LPS and nigericin co-stimulation in NR8383 cells (n = 3). Values represent mean ± SEM. Statistical comparisons were performed using one-way ANOVA. ***$P < 0.001$; ns, not significant. Fingolimod (**L**), 0.5 mg/kg; Fingolimod (**H**), 1 mg/kg.

https://doi.org/10.2147/JIR.S503428

IL-1β, IL-6, and TNF-α, as well as iNOS and p-NF-κB, in lung tissues compared with the sham group. Pulmonary inflammation is a hallmark pathological feature of ALI,[46] and elevated pro-inflammatory cytokine levels are similarly characteristic of other inflammatory lung diseases.[47–49] These findings suggest that TBI-induced pulmonary inflammation may play a crucial role in the pathogenesis of TBI-induced ALI. Several studies have reported that fingolimod and its analogs have anti-inflammatory effects that can alleviate lung injury.[28,30,50] We found that fingolimod inhibited the production of pro-inflammatory cytokines in the lungs. S1P, which is present in higher concentrations in plasma, plays a key role in regulating the endothelial barrier and vascular integrity, reducing pro-inflammatory activity, and attenuating ischemia-reperfusion injury of the lung tissues.[51] S1P treatment also improves the oxygenation capacity of lung transplant recipients. Reductions in the levels of pro-inflammatory cytokines, endothelial cell apoptosis, and neutrophil infiltration enable restoration of the endothelial barrier function.[52] In this study, fingolimod treatment led to a reduction in capillary permeability and a decreased lung wet-to-dry weight ratio post-TBI. These findings indicate that fingolimod alleviates TBI-induced ALI by suppressing pulmonary inflammation and reducing pro-inflammatory cytokine expression, which may play a key role in lung protection following TBI.

The NLRP3 inflammasome complex consists of multiple proteins that lead to the activation of caspase-1, resulting in the processing and maturation of IL-1β, a pro-inflammatory cytokine.[53] TBI has been demonstrated to trigger severe TBI-induced ALI through the induction of pulmonary cell death.[15] IL-1β is capable of upregulating IL-6, TNF-α, and other inflammatory mediators.[54] Overly high levels of inflammatory mediators are central to the pathogenesis of TBI-induced ALI.[55] The present study demonstrated that fingolimod effectively suppresses pulmonary NLRP3 inflammasome activity, thereby mitigating the onset of ALI. Given its promising anti-inflammatory properties, fingolimod may serve as a potential therapeutic strategy for TBI management.

ROS are produced as a consequence of normal oxygen metabolism.[56] When they accumulate at an excessive level, however, these free radicals can disrupt normal redox homeostasis, which can trigger inflammation and associated disease.[54] ROS signaling upstream of the NLRP3 inflammasome is thought to trigger a ROS/MAPKs/NF-κB/NLRP3 signaling axis.[57] After TBI, the induction of oxidative stress can lead to the dysfunction of the mitochondria, the deterioration of the BBB, sensorimotor dysfunction, and the emergence of brain edema that is secondary to neuronal damage.[58] Overly high levels of pulmonary oxidative stress and inflammation have been established as potential mediators of TBI-induced ALI pathogenesis.[11] In the present study, pulmonary ROS levels were significantly elevated in TBI model rats compared to sham controls, while fingolimod administration effectively attenuated these increases. In in vitro experiments, NR8383 cells were treated with LPS and nigericin to simulate prolonged NLRP3 inflammasome activation and oxidative stress. This treatment led to increased ROS accumulation and upregulated NLRP3 inflammasome signaling. However, fingolimod significantly suppressed both NLRP3 activation and ROS production, restoring oxidative balance. These findings suggest that fingolimod mitigates NLRP3 inflammasome activation by reducing oxidative stress, highlighting its potential as a therapeutic intervention for TBI-induced ALI.

Limitations

The study has several limitations. First, the precise mechanistic basis underlying the therapeutic benefits of fingolimod in treating TBI-induced ALI remains to be fully elucidated. Further studies are required to explore other potential mechanisms, such as the role of mitochondrial oxidative stress and the involvement of alternative inflammasome complexes. TBI has been reported to activate the AIM2 and NLRP1 inflammasomes,[59] and NLRP3 inhibition may be modulated by multiple pathways, including calcium channel signaling, the NF-κB pathway, and the PI3K/AKT/mTOR pathway.[60] Future studies should specifically assess the activation of these inflammasomes in the lungs following TBI and determine the extent to which fingolimod influences these pathways. Fingolimod is currently undergoing evaluation in clinical trials and has demonstrated efficacy in treating various diseases, supporting its potential safety and utility as a therapeutic agent for TBI.[61] Although the findings of this study offer valuable translational insights, further validation in a clinical setting is essential to confirm the therapeutic relevance of fingolimod.

Conclusion

In summary, fingolimod effectively suppresses NLRP3 inflammasome activation by mitigating oxidative stress, thereby protecting against TBI-induced ALI. These findings highlight the potential of fingolimod as a novel therapeutic strategy for this severe complication of TBI while also providing new insights into the underlying pathophysiological mechanisms of the disease.

Abbreviations

ALI, Acute Lung Injury; TBI, Traumatic Brain Injury; NLRP3, Nucleotide-Binding Oligomerisation Domain-Like Receptor Family Pyrin Domain Containing 3; BBB, Blood Brain Barrier; ASC, Apoptosis-Associated Speck-Like Protein Containing a Caspase-Recruitment Domain; IL-1β, Interleukin-1β; LPS, Lipopolysaccharide; ROS, Reactive Oxygen Species; CNS, Central Nervous System; NPE, Neurogenic Pulmonary Edema; NOD, Nucleotide-Binding Oligomerisation Domain; S1P, Sphingosine-1-Phosphate; FDA, Food and Drug Administration; DHE, Dihydroethidium; DAB, Diaminobenzidine; RIPA, Radio Immunoprecipitation Assay; TUNEL, Terminal Deoxynucleotidyl Transferase dUTP Nick-End Labeling; BSA, Bovine Serum Albumin; DAPI, 4′,6-Diamidino-2-Phenylindole; ELISA, Enzyme-Linked Immunosorbent Assay; TNF-α, Tumor Necrosis Factor-α; IL-6, Interleukin-6; HE, Hematoxylin and Eosin; BALF, Bronchoalveolar Lavage Fluid; IHC, Immunohistochemical; NR8383, Rats Alveolar Macrophage Cells; DCFH-DA, 2′,7′-Dichlorofluorescin Diacetate; AIM2, Absent in Melanoma 2.

Data Sharing Statement

The data and materials that support the findings of this study are available from the corresponding author upon reasonable request.

Acknowledgments

This work was supported by Tianjin Health Science and Technology Project Key Discipline Special Project (TJWJ2022XK031), Tianjin Key Medical Discipline (Specialty) Construction Project (TJYXZDXK-022A), Tianjin Jinnan District Science and Technology Plan Project (20220104), and the Scientific Research Program of Tianjin Municipal Education Commission (2023KJ063). The graphical abstract was created with BioRender.com.

Author Contributions

All authors made a significant contribution to the work reported, whether that is in the conception, study design, execution, acquisition of data, analysis, and interpretation, or all these areas; took part in drafting, revising, or critically reviewing the article; gave final approval of the version to be published; have agreed on the journal to which the article has been submitted; and agree to be accountable for all aspects of the work.

Disclosure

The authors report no conflicts of interest in this work.

References

1. Han X, Zhou H. Monitoring traumatic brain injury in China. *Lancet Neurol*. 2019;18(9):813. doi:10.1016/S1474-4422(19)30237-6
2. Dewan MC, Rattani A, Gupta S, et al. Estimating the global incidence of traumatic brain injury. *J Neurosurg*. 2019;130(4):1080–1097. doi:10.3171/2017.10.JNS17352
3. Maas AIR, Menon DK, Adelson PD, et al. Traumatic brain injury: integrated approaches to improve prevention, clinical care, and research. *Lancet Neurol*. 2017;16(12):987–1048. doi:10.1016/S1474-4422(17)30371-X
4. Das M, Mohapatra S, Mohapatra SS. New perspectives on central and peripheral immune responses to acute traumatic brain injury. *J Neuroinflammation*. 2012;9:236. doi:10.1186/1742-2094-9-236
5. Li C, Chen W, Lin F, et al. Functional two-way crosstalk between brain and lung: the brain-lung axis. *Cell mol Neurobiol*. 2023;43(3):991–1003. doi:10.1007/s10571-022-01238-z
6. Mascia L. Acute lung injury in patients with severe brain injury: a double hit model. *Neurocrit Care*. 2009;11(3):417–426. doi:10.1007/s12028-009-9242-8

7. Kerr NA, de Rivero Vaccari JP, Weaver C, et al. Enoxaparin attenuates acute lung injury and inflammasome activation after traumatic brain injury. *J Neurotrauma*. 2021;38(5):646–654. doi:10.1089/neu.2020.7257
8. Rincon F, Ghosh S, Dey S, et al. Impact of acute lung injury and acute respiratory distress syndrome after traumatic brain injury in the United States. *Neurosurgery*. 2012;71(4):795–803. doi:10.1227/NEU.0b013e3182672ae5
9. Kim JT, Song K, Han SW, et al. Modeling of the brain-lung axis using organoids in traumatic brain injury: an updated review. *Cell Biosci*. 2024;14(1):83. doi:10.1186/s13578-024-01252-2
10. Busl KM, Bleck TP. Neurogenic pulmonary edema. *Crit Care Med*. 2015;43(8):1710–1715. doi:10.1097/CCM.0000000000001101
11. Xu X, Zhi T, Chao H, et al. ERK1/2/mTOR/Stat3 pathway-mediated autophagy alleviates traumatic brain injury-induced acute lung injury. *Biochim Biophys Acta Mol Basis Dis*. 2018;1864(5 Pt A):1663–1674. doi:10.1016/j.bbadis.2018.02.011
12. Chen L, Cao SQ, Lin ZM, He SJ, Zuo JP. NOD-like receptors in autoimmune diseases. *Acta Pharmacol Sin*. 2021;42(11):1742–1756. doi:10.1038/s41401-020-00603-2
13. Hu Y, Mao K, Zeng Y, et al. Tripartite-motif protein 30 negatively regulates NLRP3 inflammasome activation by modulating reactive oxygen species production. *J Immunol*. 2010;185(12):7699–7705. doi:10.4049/jimmunol.1001099
14. Li F, Qin N, Yu Y, et al. TREM-1 inhibition or ondansetron administration ameliorates NLRP3 inflammasome and pyroptosis in traumatic brain injury-induced acute lung injury. *Arch Med Sci*. 2024;20(3):984–996. doi:10.5114/aoms/174264
15. Li TT, Sun T, Wang YZ, Wan Q, Li WZ, Yang WC. Molecular hydrogen alleviates lung injury after traumatic brain injury: pyroptosis and apoptosis. *Eur J Pharmacol*. 2022;914:174664. doi:10.1016/j.ejphar.2021.174664
16. Kerr NA, de Rivero Vaccari JP, Abbassi S, et al. Traumatic brain injury-induced acute lung injury: evidence for activation and inhibition of a neural-respiratory-inflammasome axis. *J Neurotrauma*. 2018;35(17):2067–2076. doi:10.1089/neu.2017.5430
17. Shao XF, Li B, Shen J, et al. Ghrelin alleviates traumatic brain injury-induced acute lung injury through pyroptosis/NF-kappaB pathway. *Int Immunopharmacol*. 2020;79:106175. doi:10.1016/j.intimp.2019.106175
18. Zhang L, Jiang YH, Fan C, et al. MCC950 attenuates doxorubicin-induced myocardial injury in vivo and in vitro by inhibiting NLRP3-mediated pyroptosis. *Biomed Pharmacother*. 2021;143:112133. doi:10.1016/j.biopha.2021.112133
19. Schwaid AG, Spencer KB. Strategies for targeting the NLRP3 inflammasome in the clinical and preclinical space. *J Med Chem*. 2021;64(1):101–122. doi:10.1021/acs.jmedchem.0c01307
20. Chun J, Kihara Y, Jonnalagadda D, Blaho VA. Fingolimod: lessons learned and new opportunities for treating multiple sclerosis and other disorders. *Annu Rev Pharmacol Toxicol*. 2019;59:149–170. doi:10.1146/annurev-pharmtox-010818-021358
21. Rolland WB, Lekic T, Krafft PR, et al. Fingolimod reduces cerebral lymphocyte infiltration in experimental models of rodent intracerebral hemorrhage. *Exp Neurol*. 2013;241:45–55. doi:10.1016/j.expneurol.2012.12.009
22. Wei Y, Yemisci M, Kim HH, et al. Fingolimod provides long-term protection in rodent models of cerebral ischemia. *Ann Neurol*. 2011;69(1):119–129. doi:10.1002/ana.22186
23. Di Pardo A, Amico E, Favellato M, et al. FTY720 (fingolimod) is a neuroprotective and disease-modifying agent in cellular and mouse models of Huntington disease. *Hum Mol Genet*. 2014;23(9):2251–2265. doi:10.1093/hmg/ddt615
24. Hemmati F, Dargahi L, Nasoohi S, et al. Neurorestorative effect of FTY720 in a rat model of Alzheimer's disease: comparison with memantine. *Behav Brain Res*. 2013;252:415–421. doi:10.1016/j.bbr.2013.06.016
25. Gao F, Liu Y, Li X, Wang Y, Wei D, Jiang W. Fingolimod (FTY720) inhibits neuroinflammation and attenuates spontaneous convulsions in lithium-pilocarpine induced status epilepticus in rat model. *Pharmacol Biochem Behav*. 2012;103(2):187–196. doi:10.1016/j.pbb.2012.08.025
26. Norimatsu Y, Ohmori T, Kimura A, et al. FTY720 improves functional recovery after spinal cord injury by primarily nonimmunomodulatory mechanisms. *Am J Pathol*. 2012;180(4):1625–1635. doi:10.1016/j.ajpath.2011.12.012
27. Gao C, Qian Y, Huang J, et al. A three-day consecutive fingolimod administration improves neurological functions and modulates multiple immune responses of CCI mice. *mol Neurobiol*. 2017;54(10):8348–8360. doi:10.1007/s12035-016-0318-0
28. Wang L, Sammani S, Moreno-Vinasco L, et al. FTY720 (s)-phosphonate preserves sphingosine 1-phosphate receptor 1 expression and exhibits superior barrier protection to FTY720 in acute lung injury. *Crit Care Med*. 2014;42(3):e189–99. doi:10.1097/CCM.0000000000000097
29. Wang L, Letsiou E, Wang H, et al. MRSA-induced endothelial permeability and acute lung injury are attenuated by FTY720 S-phosphonate. *Am J Physiol Lung Cell mol Physiol*. 2022;322(1):L149–L161. doi:10.1152/ajplung.00100.2021
30. Shi ZA, Li TT, Kang DL, Su H, Tu FP. Fingolimod attenuates renal ischemia/reperfusion-induced acute lung injury by inhibiting inflammation and apoptosis and modulating S1P metabolism. *J Int Med Res*. 2021;49(8):3000605211032806. doi:10.1177/03000605211032806
31. Malhotra S, Hurtado-Navarro L, Pappolla A, et al. Increased NLRP3 inflammasome activation and pyroptosis in patients with multiple sclerosis with fingolimod treatment failure. *Neurol Neuroimmunol Neuroinflamm*. 2023;10(3). doi:10.1212/NXI.0000000000200100
32. Komnig D, Dagli TC, Habib P, Zeyen T, Schulz JB, Falkenburger BH. Fingolimod (FTY720) is not protective in the subacute MPTP mouse model of parkinson's disease and does not lead to a sustainable increase of brain-derived neurotrophic factor. *J Neurochem*. 2018;147(5):678–691. doi:10.1111/jnc.14575
33. Guo Y, Gan X, Zhou H, et al. Fingolimod suppressed the chronic unpredictable mild stress-induced depressive-like behaviors via affecting microglial and NLRP3 inflammasome activation. *Life Sci*. 2020;263:118582. doi:10.1016/j.lfs.2020.118582
34. Huang L, Kang J, Chen G, et al. Low-intensity focused ultrasound attenuates early traumatic brain injury by OX-A/NF-kappaB/NLRP3 signaling pathway. *Aging*. 2022;14(18):7455–7469. doi:10.18632/aging.204290
35. Matute-Bello G, Downey G, Moore BB, et al. An official American thoracic society workshop report: features and measurements of experimental acute lung injury in animals. *Am J Respir Cell mol Biol*. 2011;44(5):725–738. doi:10.1165/rcmb.2009-0210ST
36. Qian Y, Gao C, Zhao X, et al. Fingolimod attenuates lung injury and cardiac dysfunction after traumatic brain injury. *J Neurotrauma*. 2020;37(19):2131–2140. doi:10.1089/neu.2019.6951
37. Feng D, Liu T, Zhang X, et al. Fingolimod improves diffuse brain injury by promoting AQP4 polarization and functional recovery of the glymphatic system. *CNS Neurosci Ther*. 2024;30(3):e14669. doi:10.1111/cns.14669
38. Zhang Z, Fauser U, Schluesener HJ. Early attenuation of lesional interleukin-16 up-regulation by dexamethasone and FTY720 in experimental traumatic brain injury. *Neuropathol Appl Neurobiol*. 2008;34(3):330–339. doi:10.1111/j.1365-2990.2007.00893.x
39. Zhang Z, Zhang Z, Fauser U, Artelt M, Burnet M, Schluesener HJ. FTY720 attenuates accumulation of EMAP-II+ and MHC-II+ monocytes in early lesions of rat traumatic brain injury. *J Cell Mol Med*. 2007;11(2):307–314. doi:10.1111/j.1582-4934.2007.00019.x

40. Pournajaf S, Dargahi L, Javan M, Pourgholami MH. Molecular pharmacology and novel potential therapeutic applications of fingolimod. *Front Pharmacol*. 2022;13:807639. doi:10.3389/fphar.2022.807639
41. Fu Y, Zhang N, Ren L, et al. Impact of an immune modulator fingolimod on acute ischemic stroke. *Proc Natl Acad Sci U S A*. 2014;111 (51):18315–18320. doi:10.1073/pnas.1416166111
42. Fu Y, Hao J, Zhang N, et al. Fingolimod for the treatment of intracerebral hemorrhage: a 2-arm proof-of-concept study. *JAMA Neurol*. 2014;71 (9):1092–1101. doi:10.1001/jamaneurol.2014.1065
43. Li X, Deng J, Long Y, et al. Focus on brain-lung crosstalk: preventing or treating the pathological vicious circle between the brain and the lung. *Neurochem Int*. 2024;178:105768. doi:10.1016/j.neuint.2024.105768
44. Ziaka M, Exadaktylos A. Brain-lung interactions and mechanical ventilation in patients with isolated brain injury. *Crit Care*. 2021;25(1):358. doi:10.1186/s13054-021-03778-0
45. Demling R, Riessen R. Pulmonary dysfunction after cerebral injury. *Crit Care Med*. 1990;18(7):768–774. doi:10.1097/00003246-199007000-00019
46. Matthay MA, Arabi Y, Arroliga AC, et al. A new global definition of acute respiratory distress syndrome. *Am J Respir Crit Care Med*. 2024;209 (1):37–47. doi:10.1164/rccm.202303-0558WS
47. Businaro R, Maggi E, Armeli F, Murray A, Laskin DL. Nutraceuticals as potential therapeutics for vesicant-induced pulmonary fibrosis. *Ann N Y Acad Sci*. 2020;1480(1):5–13. doi:10.1111/nyas.14442
48. Hommes TJ, Hoogendijk AJ, Dessing MC, et al. Triggering receptor expressed on myeloid cells-1 (TREM-1) improves host defence in pneumococcal pneumonia. *J Pathol*. 2014;233(4):357–367. doi:10.1002/path.4361
49. Lentsch AB, Czermak BJ, Bless NM, Ward PA. NF-kappaB activation during IgG immune complex-induced lung injury: requirements for TNF-alpha and IL-1beta but not complement. *Am J Pathol*. 1998;152(5):1327–1336.
50. Qian J, Ye Y, Lv L, Zhu C, Ye S. FTY720 attenuates paraquat-induced lung injury in mice. *Int Immunopharmacol*. 2014;21(2):426–431. doi:10.1016/j.intimp.2014.05.025
51. Stone ML, Sharma AK, Zhao Y, et al. Sphingosine-1-phosphate receptor 1 agonism attenuates lung ischemia-reperfusion injury. *Am J Physiol Lung Cell mol Physiol*. 2015;308(12):L1245–52. doi:10.1152/ajplung.00302.2014
52. Okazaki M, Kreisel F, Richardson SB, et al. Sphingosine 1-phosphate inhibits ischemia reperfusion injury following experimental lung transplantation. *Am J Transplant*. 2007;7(4):751–758. doi:10.1111/j.1600-6143.2006.01710.x
53. Tschopp J, Schroder K. NLRP3 inflammasome activation: the convergence of multiple signalling pathways on ROS production? *Nat Rev Immunol*. 2010;10(3):210–215. doi:10.1038/nri2725
54. Kelley N, Jeltema D, Duan Y, He Y. The NLRP3 inflammasome: an overview of mechanisms of activation and regulation. *Int J mol Sci*. 2019;20 (13):3328. doi:10.3390/ijms20133328
55. Dai SS, Wang H, Yang N, et al. Plasma glutamate-modulated interaction of A2AR and mGluR5 on BMDCs aggravates traumatic brain injury-induced acute lung injury. *J Exp Med*. 2013;210(4):839–851. doi:10.1084/jem.20122196
56. Zorov DB, Juhaszova M, Sollott SJ. Mitochondrial reactive oxygen species (ROS) and ROS-induced ROS release. *Physiol Rev*. 2014;94 (3):909–950. doi:10.1152/physrev.00026.2013
57. An Y, Zhang H, Wang C, et al. Activation of ROS/MAPKs/NF-kappaB/NLRP3 and inhibition of efferocytosis in osteoclast-mediated diabetic osteoporosis. *FASEB J*. 2019;33(11):12515–12527. doi:10.1096/fj.201802805RR
58. Fesharaki-Zadeh A. Oxidative stress in traumatic brain injury. *Int J mol Sci*. 2022;23(21):13000. doi:10.3390/ijms232113000
59. Freeman LC, Ting JP. The pathogenic role of the inflammasome in neurodegenerative diseases. *J Neurochem*. 2016;136 Suppl 1:29–38. doi:10.1111/jnc.13217
60. Zhou R, Yazdi AS, Menu P, Tschopp J. A role for mitochondria in NLRP3 inflammasome activation. *Nature*. 2011;469(7329):221–225. doi:10.1038/nature09663
61. Bascunana P, Mohle L, Brackhan M, Pahnke J. Fingolimod as a treatment in neurologic disorders beyond multiple sclerosis. *Drugs R D*. 2020;20 (3):197–207. doi:10.1007/s40268-020-00316-1